A Shell Finite Element Model of the Pelvic Floor Muscles

D. d'Aulignac*, J.A.C. Martins*, T. Mascarenhas†, R.M. Natal Jorge‡, and E.B. Pires*

Abstract

The pelvic floor gives support to the organs in the abdominal cavity. Using the dataset made public in [11] we have reconstructed the geometry of one of the most important parts of the pelvic floor, the levator ani, using NURB surfaces. Once the surface is triangulated, this mesh is used in a finite element analysis with shell elements.

Based on the 3D behavior of the muscle we have constructed a shell that takes into account the direction of the muscle fibers and the incompressibility of the tissue. The constitutive model for the isotropic strain energy and the passive strain energy stored in the fibers are adapted from Humphrey's model for cardiac muscles. To this the active behavior of the skeletal muscle is added.

We present preliminary results of a simulation of the levator ani muscle under pressure and with active contraction. This research aims at helping predict the damages to the pelvic floor that can occur during childbirth.

1 Introduction

The pelvic floor is a large sling or hammock that stretches from side to side of the pelvis to support the pelvic organs and abdominal contents. The mechanism of support involves the interconnections of several structures:

1. the arcus tendinus is a fibrous band that is attached in the front to the pubic bone and in the back to the ischial spine;

2. the levator ani provides support for the urethra, vagina and rectum; it is made up of type I, slow twitch muscle fibers and Type II, fast twitch muscle fibers; at least 80 percent of the levator ani are Type I fibers that produce less force on contraction, but are also fatigue resistant;

3. the endopelvic fascia that connects the pelvic organs.

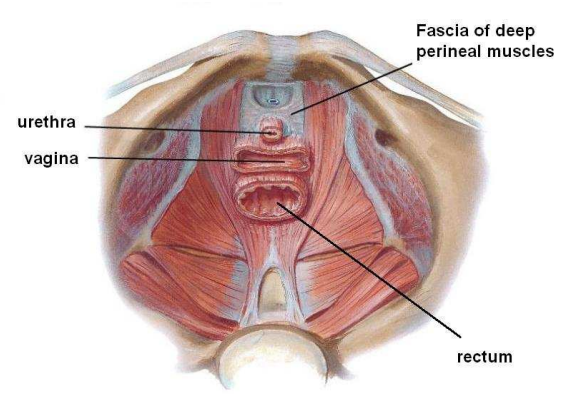

Figure 1: Anatomical drawing of the levator ani muscle.

The opening within the levator ani muscle through which the urethra and vagina pass, is called the urogenital hiatus. The rectum also passes through this opening, but because the levator ani muscles attach directly to the anus it is not included in the name of the hiatus. The hiatus, therefore, is bounded anteriorly by the pubic bones, laterally by the levator ani muscles, and posteriorly by the perineal body and the anal sphincter. The normal baseline activity of the levator ani muscle keeps the urogenital hiatus closed. It squeezes the vagina, urethra, and rectum closed by compressing them against the pubic bone and lifts the floor and organs in an upward direction [2].

2 Geometrical Model

Due to the thin nature of the levator ani muscle it is very difficult to construct geometrical models of the pelvic floor from MRI or CT data. Although this has been done successfully in the past for visu-

*Departamento de Engenharia Civil e ICIST, Instituto Superior Técnico, Av. Rovisco Pais, 1049-001 Lisboa, Portugal, e-mail: {diego,jmartins,bpires}@civil.ist.utl.pt, web: http://www.civil.ist.utl.pt/icist

†Hospital de São João, Departamento de Ginecologia e Obstetrícia, Faculdade de Medicina, Universidade do Porto, Porto, Portugal

‡IDMEC, Faculty of Engineering, University of Porto, Portugal

Figure 2: MRI image of the pelvis.

alization purposes [16, 9], we felt that these models were inadequate for a finite element simulation, because of the meshes used.

Hence, we have preferred to use the geometrical point data obtained from cadaver measurements by Janda et al [11] to reconstruct the surface of the levator ani muscle. All measurements were performed on one embalmed 72 year old female cadaver obtained for scientific research with no known pathologies of the pelvic floor. The result is a 3D point-set of the pelvic floor that is publically available on the internet[1].

We constructed a surface from this point-set in two consecutive steps. Firstly, the edges of the muscles are defined using splines. Afterwards, from these splines, NURBS surfaces are created using the Rhino[2] software. Once triangulated, these surfaces provide a good geometrical model for a FEM simulation.

3 Physical Muscle Model

Since the pelvic floor is very thin (approximately $2mm$), the 3D model developed in [14] for the active and passive behavior of the muscle has been modified in accordance to the theory of shells. The Cauchy stress for the 3D material is given as

$$\sigma = \frac{1}{J}\text{dev}\left[2U_I' B + U_f' \lambda_f (n \otimes n)\right] + pI, \qquad (1)$$

where

$$U_I' = \frac{\partial U_I}{\partial I_1^C}$$

is the change in strain energy stored in the isotropic matrix ,

$$U_f' = \frac{\partial U_f}{\partial \lambda_f}$$

is the change in strain energy stored in the muscle fibers, p is the pressure, and

$$\text{dev}[\cdot] = (\cdot) - \frac{1}{3}\text{tr}(\cdot)I.$$

In the case of a shell the deformation gradient F is given by

$$F = \begin{bmatrix} F_{11} & F_{12} & 0 \\ F_{21} & F_{22} & 0 \\ 0 & 0 & F_{33} \end{bmatrix} = \begin{bmatrix} F_p & 0 \\ 0 & F_{33} \end{bmatrix},$$

where the direction 3 of the orthonormal reference frame (1,2,3) follows the normal to the middle surface of the shell. As we assume perfect incompressibility, $J = \det F$ will always be equal to 1. Hence,

$$F_{33} = \frac{1}{\det F_p}.$$

Therefore, the left and right Cauchy-Green tensors are given as

$$B = \begin{bmatrix} F_p F_p^T & 0 \\ 0 & F_{33}^2 \end{bmatrix}, C = \begin{bmatrix} F_p^T F_p & 0 \\ 0 & F_{33}^2 \end{bmatrix}.$$

The first invariant can then be calculated as

$$I_1^C = \text{tr}(C_p) + C_{33},$$

and the strain in the direction of the fibers is

$$\lambda_f = \sqrt{N_p^T C_p N_p},$$

where N_p is the direction of the fibers in the undeformed state. Then n_p will be the direction of the fibers in the deformed configuration:

$$n_p = \frac{F_p N_p}{\lambda_f}.$$

Hence, from Equation 1, given that σ_{33} must be equal to zero, the pressure has to be

$$p = \frac{1}{3}\left[2U_I'(\text{tr}(B_p) - 2B_{33}) + \lambda_f U_f'\right]. \qquad (2)$$

Therefore, the Cauchy stress in the plane is given as

$$\sigma_p = 2U_I'(B_p - B_{33}I_p) + \lambda_f U_f'(n_p \otimes n_p) \qquad (3)$$

By differentiation the rate of the Cauchy stress tensor is

[1] http://www.wbmt.tudelft.nl/mms/morph_data/
[2] http://www.rhino3d.com

$$\begin{aligned}\dot{\sigma}_p =& 2U_I'' \dot{I}_1^C (B_p - B_{33} I_p) \\ &+ 2U_I' (\dot{B}_p - \dot{B}_{33} I_p) \\ &+ \dot{\lambda}_f U_f' (n_p \otimes n_p) \\ &+ \lambda_f U_f'' \dot{\lambda}_f (n_p \otimes n_p) \\ &+ \lambda_f U_f' (\dot{n}_p \otimes n_p + n_p \otimes \dot{n}_p)\end{aligned} \tag{4}$$

and the rate of the deformation gradient is given as

$$\dot{F} = LF = \begin{bmatrix} L_p F_p & 0 \\ 0 & L_{33} F_{33} \end{bmatrix}.$$

Further, the spatial velocity gradient L can be decomposed into

$$L = (D + W),$$

where D is the rate of deformation tensor and W the spin tensor. By substitution we then obtain.

$$\dot{F} = \begin{bmatrix} (D_p + W_p) F_p & 0 \\ 0 & D_{33} F_{33} \end{bmatrix}.$$

Therefore, since $D_{33} = -(D_{11} + D_{22})$,

$$\dot{F}_{33} = D_{33} F_{33} = -\frac{(D_{11} + D_{22})}{\det F_p}.$$

Further, the rate of the left Cauchy-Green tensor is given as

$$\begin{aligned}\dot{B}_p &= \dot{F}_p F_p^T + F_p \dot{F}_p^T \\ &= L_p F_p F_p^T + F_p F_p^T L_p^T,\end{aligned}$$

and the rate of the right Cauchy-Green tensor is

$$\begin{aligned}\dot{C}_p &= \dot{F}_p^T F_p + F_p^T \dot{F}_p \\ &= F_p^T L_p^T F_p + F_p^T L_p F_p.\end{aligned}$$

Since B_{33} and C_{33} are the same, their rate of change is also equal

$$\dot{B}_{33} = \dot{C}_{33} = \frac{\partial C_{33}}{\partial F_{33}} \dot{F}_{33} = 2 F_{33} \dot{F}_{33}.$$

Hence, the change of the first invariant can then be calculated as

$$\dot{I}_1^C = \mathrm{tr}(\dot{C}_p) + \dot{C}_{33},$$

and the strain rate in the direction of the fibers is

$$\dot{\lambda}_f = \lambda_f (n_p^T D_p n_p),$$

where n_p is the direction of the fibres in the deformed configuration and its derivative is given by

$$\dot{n}_p = \left[L - (n_p^T D_p n_p) I_p \right] n_p.$$

Finally, the Jacobian of the Cauchy stress tensor is given as

$$\frac{\partial \Delta \sigma_p}{\partial \Delta \epsilon_p} = \frac{\partial \dot{\sigma}_p}{\partial D_p}, \tag{5}$$

and an estimate of the shell transverse shear stiffness at $F = I$, as required by the ABAQUS software, is

$$K_{11}^{ts} = K_{22}^{ts} = \left[\frac{1}{6} \left(\frac{\partial \dot{\sigma}_{11}}{\partial D_{11}} + \frac{\partial \dot{\sigma}_{22}}{\partial D_{22}} \right) + \frac{1}{3} \frac{\partial \dot{\sigma}_{12}}{\partial D_{12}} \right] t$$

where t is the thickness of the shell.

3.1 Active muscle contraction

Much of the research into the contraction of skeletal muscles has focused on their 1D behavior along the fibers. Probably, the most well known of the proposed models is the Hill muscle model [5]. These models have allowed to simulate successfully complex human movements [4]. However, more recently, the simulation of 3D muscles models is being considered [14, 15].

Our approach assumes that the strain energy is stored isotropically in the material as well as in the direction of the muscle fibers:

$$U = U_I(I_1^C) + U_f(\lambda_f, \alpha). \tag{6}$$

Further, the strain energy stored in the muscle fibers can be divided into a passive elastic part and an active part due to the contraction.

$$U_f(\lambda_f, \alpha) = U_{pas}(\lambda_f) + U_{act}(\lambda_f, \alpha), \tag{7}$$

where α is the activation level ranging from 0 to 1.

4 Results

4.1 Passive stretching

For the passive behavior of the muscle we use the constitutive equation proposed by Humphrey and Yin [10] for the deformation of cardiac muscle tissues. Hereby, the isotropic strain energy stored is given as

$$U_I = c\{\exp[b(I_1^C - 3)] - 1\}, \tag{8}$$

and the passive strain energy stored in the fibers is

$$U_{pas} = A\{\exp[a(\lambda_f - 1)^2] - 1\} \tag{9}$$

when $\lambda_f > 1$. Otherwise we consider the strain energy to be zero, assuming that the fibers offer no resistance to compression.

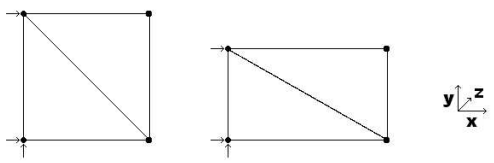

Figure 3: The fibers are all aligned along the x direction. Strains along the fibers are imposed, but the material is free to deform in the y direction.

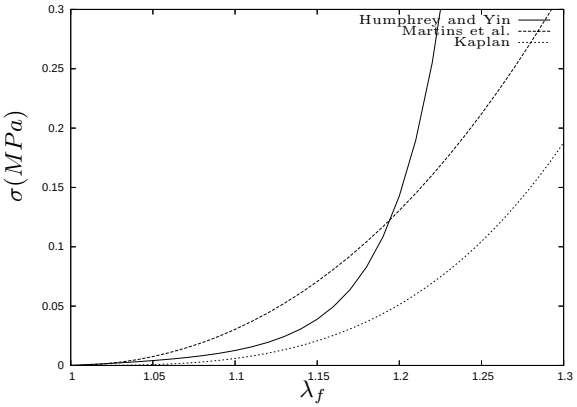

Figure 4: Test for the passive stretch of a shell in the in the direction of the fibers using the Humphrey and Yin [10] model, the Martins et al. [14] model, and compared to the 1D model given by Kaplan [12].

In an example test we consider a square shell with dimensions $1cm$ along the sides and $1mm$ thickness. The shell is meshed using two triangular elements. The fibers are all aligned along the x direction and the material is then stretched along the direction of the fibers, but is allowed to deform freely perpendicularly (see also Figure 3). The parameters for Humphrey and Yin's equations (Equations 8 and 9) are: $c = 0.394kPa, b = 23.46, A = 0.595kPa, a = 12.43$.

The results obtained for the normal Cauchy stress component along the direction of the fibers are plotted in Figure 4. However, large quantitative differences can be observed when comparing this model to others, like the one used in [14] or the 1D model given by Kaplan [12] for example. Hence it will be essential to compare these models with experimental data for validation.

Further, an important question remains unanswered: how much of the total passive stress is due to the isotropic stress, and how much due to the contribution of the fibers? In Martins et al., based on the in vitro experiments by [8], the isotropic stresses are very small with respect

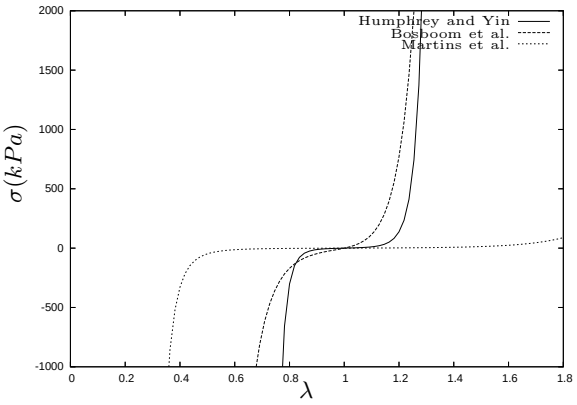

Figure 5: Comparison of the isotropic stresses of the Humphrey and Yin [10], Martins et al. [14], and Bosboom et al. [3]

to the stresses produced by the fibers. On the other hand, Humphrey and Yin suggest that the isotropic stresses are larger than those produced by the fibers. Finally, an Ogden material with the parameters given by Bosboom et al. [3] (based on an in vivo experiment of a skeletal muscle in transverse compression) may be softer than Humphrey and Yin's model in compression, but even stiffer in extension.

4.2 Active Contraction

The maximum isometric tension a muscle can generate depends strongly on λ_f. Gordon et al [7] tested a single skeletal fiber of a frog's skeletal muscle. If λ_f is too small or too large, the tension drops to zero. The maximum tension is produced when $\lambda_f = 1$. Hence, we adopt the following equation to represent the strain energy corresponding to the active tension

$$U_{act} = \alpha T_0^M \int_1^{\lambda_f} -4(\lambda_f - 1)^2 + 1 \qquad (10)$$

for $0.5 < \lambda_f < 1.5$ where U_{act} is larger than 0. For other values of λ_f the muscle produces no force and, therefore, the strain energy is zero. Further, we choose the maximum tension produced by the muscle at resting length to be $T_0^M = 682kPa$ in accordance with values proposed in the literature.

We repeat the test performed in Section 4.1, but this time including the maximal active stress of the muscle. The total stress as a function of λ_f, i.e. isotropic stress plus passive and active stress of the fibers, is shown in Figure 6.

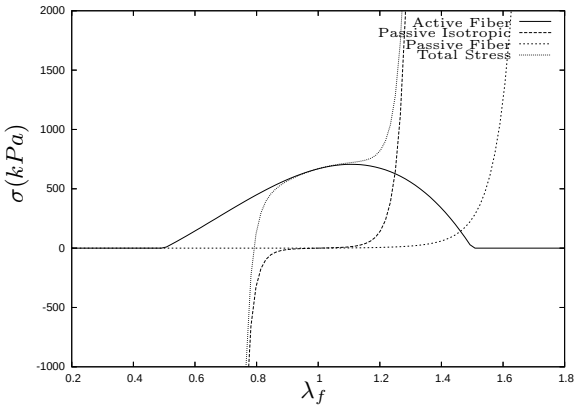

Figure 6: Total stress and its components: isotropic, passive and active stress of the fibers with respect to λ_f.

4.3 Pelvic Floor

Using the ABAQUS program we have performed numerical simulations of the deformation of the levator ani muscle when applying a pressure and contracting the muscle (see Figure 7). The levator ani is modeled using triangular S3 shell elements and the muscle material has been defined by implementing a UMAT routine in FORTRAN.

We assume that the nodes connected to the pelvic bone, ligament, and coccyx are fixed in translation but free in rotation. All other nodes are free.

The initial direction of the fibers is chosen in the direction of the maximum principal stress in the element when applying a pressure to the muscle. This way the fibers can most effectively carry the loads applied to the pelvic floor. Medical evidence seems to corroborate this alignment.

It is interesting to note that when the muscle is passively submitted to a pressure the regions of maximum stress occur at the sling attachment points of the levator ani, where most post-partum lesions occur.

5 Discussion and Future Work

For any realistic simulation an accurate description of the properties of the modeled material is of paramount importance. However, we discovered large quantitative differences between existing models and parameters used [6, 13, 14, 15]. Hence, it will be essential to compare these models with each other as well as with experimental data available.

The pelvic floor is an extremely complicated structure from a bio-mechanical point of view. It

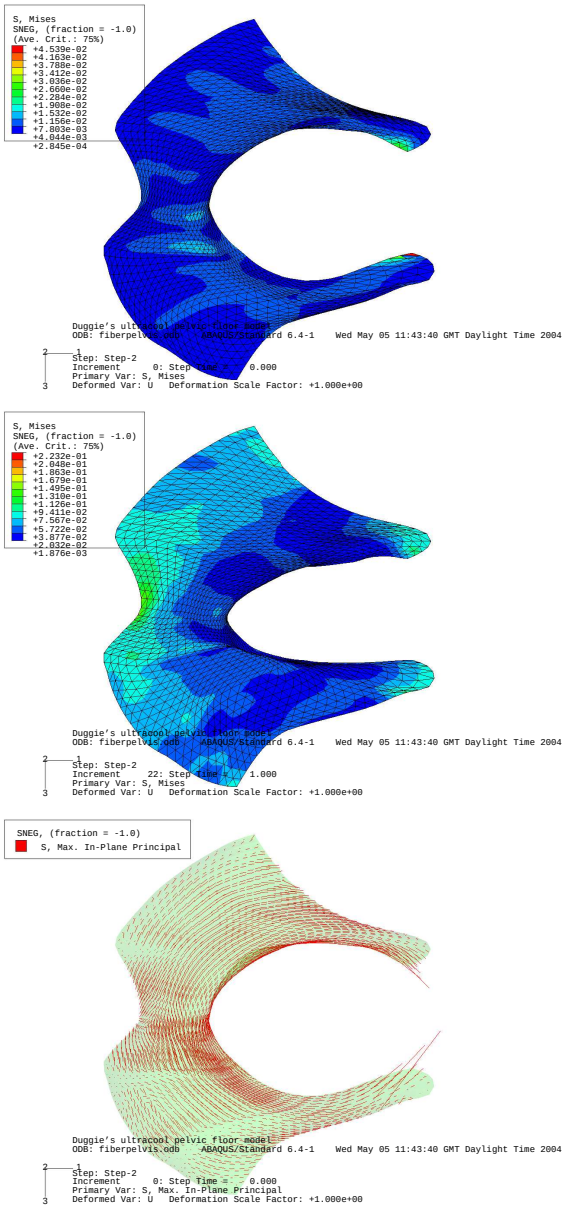

Figure 7: Finite element simulation of the pelvic floor: axial view under pressure (top) and with active contraction (middle). The bottom picture shows the fiber alignment along the principal stress vector. Animations may be found on http://www.civil.ist.utl.pt/~diego/work/publi.html

is composed of muscles and ligaments, and is intrinsically linked to the supported organs. The exact modeling of all structures and their interactions with each other is indeed a very challenging problem. Hence, we believe, it is advisable to isolate a smaller, more manageable problem against which we can validate our assumptions.

Of course, to be of any practical importance, the geometry (and possibly the material properties) will have to be calibrated on the patient. Since the anatomy of every patient is different, possibly the best way would be to use data from MRI images. Once the pelvic floor is segmented it would then be feasible to construct a geometrical model based on this information.

In this study we have used shell elements because of the thin nature of the levator ani muscle. However, this muscle is connected to other structures like the rectum or the vagina that would more adequately be modeled by volumetric elements. One possibility would be the use of special 8-node brick element suitable for thin structures [1].

Finally, we hope that an accurate model of the pelvic floor will allow a simplified simulation of childbirth, allowing doctors to make an informed decision on whether a cesarean or vaginal delivery is most advisable for the patient.

Acknowledgments

This work is part of the project "New materials, adaptive systems and their nonlinearities; modelling control and numerical simulation" carried out in the framework of the European community program "Improving the human research potential and the socio-economic knowledge base" (Contract N° HPRN-CT-2002-00284).

References

[1] R.J. Alves de Sousa, R.M. Natal Jorge, R.A. Fontes Valente, and J.M.A. César de Sá. A new volumetric and shear locking-free 3d enhanced strain element. *Engineering Computations*, 20(7):896–925, 2003.

[2] C.I. Bartram and J.O.L. DeLancey, editors. *Imaging Pelvic Floor Disorders*. Springer Verlag, 2003.

[3] E.M.H. Bosboom, M.K.C. Hesselink, C.W.J. Oomens, C.V.C Bouten, M.R. Drost, and F.P.T Baaijens. Passive transverse mechanical properties of skeletal muscle under in vivo compression. *Journal of Biomechanics*, 34:1365–1368, 2001.

[4] S.L. Delp, J.P. Loan, M.G. Hoy, F.E. Zajac, E.L. Topp, and J.M Rosen. An interactive graphics-based software system to develop and analyze models of muscoskeletal structures. *IEEE Transactions on Biomedical Engineering*, 37:757–767, 1990.

[5] Y.C. Fung. *Biomechanics: Mechanical Properties of Living Tissues*. Springer Verlag, 2nd edition, 1993.

[6] A.W.J. Gielen, P.H.M. Bovendeerd, and J.D. Janssen. A finite element formulation of muscle contraction. In *DIANA Computational Mechanics*, pages 139–148, 1994.

[7] A.M. Gordon and A.F. Huxley. The variation in isometric tension with sarcomere length in vertebrate muscle fibers. *J. Physiology (London)*, 185:170–192, 1966.

[8] A.P. Grieve and C.G. Armstrong. Compressive properties of soft tissues. *Biomechanics XI-A, International Series on Biomechanics*, 1988.

[9] Lennox Hoyte, Lore Schierlitz, Kelly Zou, George Flesh, and Julia R. Fielding. Two- and 3-dimentional mri comparison of levator ani structure, volume, and integrity in women with stress incontinence and prolapse. *American Journal of Obstetrics and Gynecology*, 185(1):11–19, 2001.

[10] J.D. Humphrey and F.C.P. Yin. On constituitive relations and finite deformations of passive cardiac tissue: A pseudostrain-energy function. *ASME J. Biomech. Eng.*, 109:298–304, 1987.

[11] S. Janda, F.C.T. Van der Helm, and S.B de Blok. Measuring morphological parameters of the pelvic floor for finite element modelling purposes. *Journal of Biomechanics*, 36(6):749–757, 2003.

[12] M. L. Kaplan. *Efficient Optimal Control of Large Scale Biomechanical Systems*. PhD thesis, Stanford University, 2000.

[13] M. Kojic, S. Mijailovic, and N. Zdravkovic. Modelling of muscle behaviour by the finite element method using Hill's three-element model. *International Journal for Numerical Methods in Engineering*, 43:941–953, 1998.

[14] J.A.C. Martins, E.B. Pires, R. Salvado, and P.B. Dinis. A numerical model of passive and active behaviour of skeletal muscles. *Computer methods in applied mechanics and engineering*, 151:419–433, 1998.

[15] C.W.J. Oomens, M. Maenhout, C.H.G.A van Oijen, M.R. Drost, and F.P. Baaijens. Finite element modelling of contracting skeletal muscle. *Phil Trans R Soc Lon B*, 358:1453–1460, 2003.

[16] Russell K. Pearl, Ray Evenhouse, Mary Rasmussen, Fred Dech, Jonathan C. Silverstein, Sean Prokasky, and Walter B. Panko. The virtual pelvic floor, a tele-immersive educational environment. In *Proceedings AMIA Symposium*, pages 345–8, 1999.